HYDROLOGICAL PROCESSES
Hydrol. Process. **20**, 1827–1843 (2006)
Published online 23 December 2005 in Wiley InterScience (www.interscience.wiley.com). DOI: 10.1002/hyp.5964

Incorporating ancillary data to refine anthropogenically modified overland flow paths

Guy D. Duke, Stefan W. Kienzle,* Dan L. Johnson and James M. Byrne
University of Lethbridge, Department of Geography, 4401 University Drive, Lethbridge, Alberta T1K 4W1, Canada

Abstract:

A study carried out in the Oldman River watershed in southern Alberta, Canada, to delineate potential surface water pollution sources revealed that the use of conventional raster-based digital elevation models (DEMs) and flow-direction algorithms resulted in the delineation of incorrect watershed boundaries. The inaccuracies resulted from the resolution of the available DEM, which is too coarse to represent the presence of anthropogenically modified terrain features, such as roads, ditches and canals, which can significantly alter overland flow paths. This observation prompted the development of the computer model RIDEM (Rural Infrastructure Digital Elevation Model). By incorporating ancillary data to refine anthropogenically modified overland flow paths into the grid-based watershed delineation process, the scale of runoff flow paths created with RIDEM is reduced below the scale defined by the representation of terrain with the DEM. RIDEM also resolves the inability of grid-based flow-direction algorithms to account for the split-flow patterns that occur in irrigated landscapes. The model outputs include a corrected flow-direction matrix, gross watershed boundaries, and road-induced dead drainages. The watershed areas derived with RIDEM differed by up to 49% from watersheds derived using a conventional DEM with a 20 m grid cell size. However, results of watershed boundaries could not be verified, because highly accurate watershed boundaries do not exist for our study area. Copyright © 2005 John Wiley & Sons, Ltd.

KEY WORDS watershed; digital elevation model (DEM); downscale; overland flow path; RIDEM; hydrological modelling

INTRODUCTION

An ongoing water quality study in the Oldman River watershed Alberta, Canada, has indicated that local surface waters are occasionally contaminated with bacterial pathogens, including *Escherichia coli* O157 : H7 and *Salmonella* spp. (Hyland *et al*., 2003; Johnson *et al*., 2003; Little *et al*., 2003). The prevalence of these pathogens and other potential contaminants has prompted further investigation to assess the possible sources of contamination, including direct discharge, surface runoff and groundwater recharge. To investigate the spatial and temporal influence of watershed properties on surface water quality requires the accurate delineation of runoff transport pathways and watershed boundaries.

Automated surface-drainage derivation and watershed delineation was pioneered by O'Callaghan and Mark (1984) with the introduction of the deterministic eight-neighbour (D8) flow-direction algorithm. The D8 algorithm utilizes an orthogonal matrix of elevation values, referred to as a digital elevation model (DEM), to predict surface drainage patterns. Based on the elevations within a 3×3 grid cell window, the D8 algorithm assigns a flow direction from the central cell to the cell in which the steepest downslope path exists. Once the drainage direction is defined for all cells in the data matrix, the flow directions are connected to derive drainage networks and watershed boundaries. In addition to the D8 algorithm, other grid-based flow-direction algorithms are available: Multiple Flow Direction (Freeman, 1991; Quinn *et al*., 1991), Kinematic Routing

* Correspondence to: Stefan W. Kienzle, University of Lethbridge, Department of Geography, 4401 University Drive, Lethbridge, Alberta T1K 4W1, Canada. E-mail: stefan.kienzle@uleth.ca

Received 3 March 2004
Accepted 30 March 2005

Algorithm (Lea, 1992), Digital Elevation Model Network (DEMON; Costa-Cabral and Burges, 1994), Flux Decomposition (Desmet and Govers, 1996), D8-TOPAZ (Garbrecht and Martz, 1997), D-Infinity (Tarboton, 1997), and D8-Least Transversal Deviation (Orlandini *et al*., 2003). Because the landscape drainage patterns derived with these algorithms are based solely on elevation, their accuracy is dependent on the DEM's representation of terrain.

Raster-based DEMs are predominantly interpolated from point and/or line data with known or estimated elevation values. Many mathematical functions are available to fit a smooth surface from the sampled elevation points, such as inverse distance weighting, splining, local and global polynomial trend surfaces, kriging or specialized algorithms such as ANUDEM (Hutchinson, 1989; Hutchinson and Dowling, 1991). The terrain features represented in the DEM are conditional upon the accuracy, density, and distribution of the original point elevation data set, which is the single greatest factor affecting DEM accuracy (Gao, 1998; Gong *et al*., 2000; Huang, 2000; Kienzle, 2004). Several other factors can also influence the terrain representation of a given DEM, including the grid cell size, the roughness of the terrain surface, and the interpolation method used to derive the DEM (Gong *et al*., 2000; Huang, 2000; Kienzle, 2004).

Because the accuracy of DEM-derived drainage patterns is dependent on the accuracy of the DEM, it is crucial that the elevation values within DEMs capture the terrain features that influence drainage patterns (Jensen and Domingue, 1988). This requirement is particularly important in low-relief landscapes, where small-scale terrain features such as roads, ditches and irrigation canals can significantly affect runoff flow paths. Moore *et al*. (1991) Band and Moore (1995) and Schneider (2001) stated that imprecise landscape representation in DEMs has frequently caused the derivation of oversimplified drainage patterns in grid-based models. Beven (1995) described this as the 'scale problem', where information gained at one scale is used to make predictions at a different scale.

Landscape drainage paths are sensitive to small-scale terrain features. For example, linear landscape features as small as tillage furrows can significantly modify overland flow directions (Souchere *et al*., 1998; Cerdan *et al*., 2001; Takken *et al*., 2001a–c; Souchere *et al*., 2003). To capture small-scale sources of drainage variability such as these, it may be suggested to interpolate DEMs from data sets with point-elevation sampling intervals at metre or sub-metre scales. However, acquiring point elevations from photogrammetry at this density is impractical because the maximum density of points that can be extracted is a function of aerial photograph scale. Although light detection and ranging (LIDAR) technology can acquire points at sub-metre density, the high cost associated limits its use for smaller research areas. Recognizing the limitations of current technology, and the ineffectiveness of altering the elevation values directly (Duke *et al*., 2003), hydrological modellers have begun to incorporate ancillary data when deriving flow directions from DEMs. Saunders (2000) utilized ancillary stream data to impose or 'burn' stream vector data to improve the accuracy of flow direction matrices near streams. 'Burning' streams refers to the process of decreasing the elevation of grid cells representing watercourses to enforce the known drainage patterns on the flow-direction matrix. Takken *et al*. (2001c) developed a tillage-controlled runoff pattern algorithm that incorporates knowledge regarding tillage orientation into the Limburg Soil Erosion Model. Similarly, Cerdan *et al*. (2001) and Souchere *et al*. (2003) used the expert-based Sealing and Transfer by Runoff and Erosion related to Agricultural Management (STREAM) model to simulate erosion in agricultural watersheds. By manipulating the flow direction in tilled fields according to furrow depth and slope, and enforcing flow directions along dead furrows, the STREAM model accurately replicated the observed runoff network (Cerdan *et al*., 2001). By incorporating ancillary data into grid-based hydrological models (e.g. Saunders, 2000; Cerdan *et al*., 2001; Takken *et al*., 2001c; Duke *et al*., 2003; Souchere *et al*., 2003) the scale of the processes modelled is reduced below the scale restricted by the DEM's representation of terrain. The primary objective of these ancillary data models is to ensure that the scale of the output results matches the scale required for analysis.

The Rural Infrastructure Digital Elevation Model (RIDEM) is introduced in this paper. RIDEM enables the delineation of watersheds in areas where landscape drainage patterns have been altered by the construction of roads and irrigation canals. RIDEM implements two algorithms, namely the road enforcement algorithm (REA; Duke *et al*., 2003) and the canal enforcement algorithm (CEA). Both algorithms integrate ancillary

data to take into account anthropogenic landscape features that influence drainage patterns, but which are not represented after the interpolation of a grid-based DEM. The CEA also resolves the inability of single flow-direction algorithms to model the split-flow patterns that occur within irrigation distribution systems. Because RIDEM considers elevation values and the spatial locations of roads, irrigation canals, and cross-flow structures, e.g. siphons, flumes, and culverts, it is implemented solely for the delineation of gross watersheds and dead drainages.

CONCEPTUAL VIEW OF RURAL INFRASTRUCTURE

Roads

Duke *et al*. (2003) categorized the effects of roads on drainage patterns in low-relief landscapes in two ways. First, roads with elevated surfaces can act as barriers to overland flow, rerouting runoff on the upslope side of the road. Second, roadside ditches can create flow-path corridors on either side of the road. Both of these road profiles can also cause the formation of dead drainages. Areas upstream of these flow-path sinks contribute to stream flow through ground water recharge only. Flow-path corridors next to roads also have the potential to increase the effective drainage density when hydrologically connected to irrigation canals via culverts.

Irrigation canals

In nature, surface runoff converges from hillslopes to valleys forming progressively larger open-channel drainage networks. Several authors have made the distinction between hillslope processes that are more accurately modelled with multiple flow direction algorithms, and channel processes that are more accurately modelled with single flow direction algorithms (Freeman, 1991; Quinn *et al*., 1991; Costa-Cabral and Burges, 1994; Desmet and Govers, 1996; Gallant and Wilson, 1996; Tarboton, 1997). In contrast to natural flow patterns, irrigation canals are concentrated flow systems with split-flow patterns (Figure 1a), where flow is permitted to bifurcate into two channels (Figure 1b).

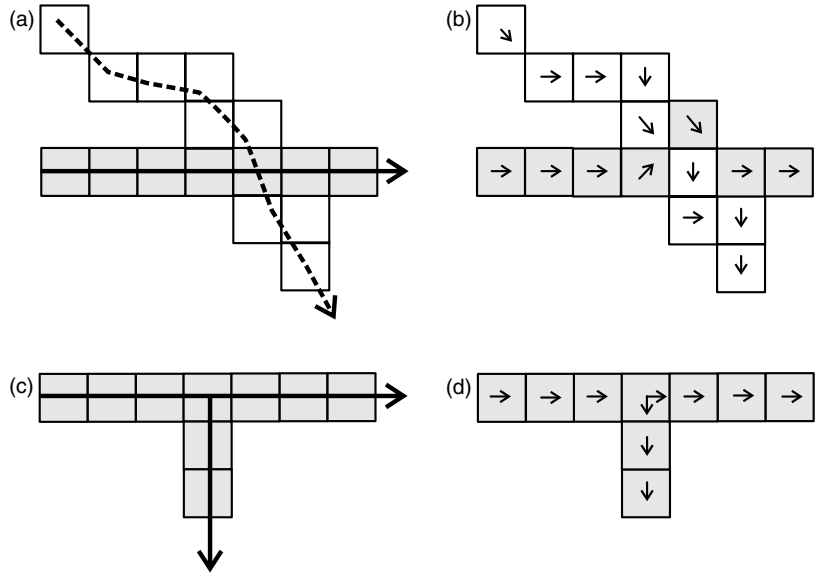

Figure 1. Flow patterns in an irrigated landscape: (a) cross-flow scenario with an irrigation canal as a solid line (raster representation shown by grey squares) and a stream course as a dotted line (white squares); (b) flow direction representation of cross-flow pattern; (c) split-flow scenario with irrigation canals as solid lines (grey squares); (d) flow direction representation of split-flow pattern

Occasionally, open channel irrigation canals are routed underneath or over drainage courses via siphons, flumes, or culverts to facilitate the natural progression of runoff and streamflow. These structures, analogous to a bridge, impose cross-flow drainage patterns that add further complexity to overland flow modelling in irrigated landscapes (Figure 1c). Cross-flow drainage patterns refer to the diagonal manipulation of flow directions in a grid-based environment to simulate the effects of these structures (Figure 1d).

MATERIALS AND METHODS

Study area

The study region extends from the fescue foothills region, situated east of the Rocky Mountains, to the low-relief dry mixed-grass region with both dryland and irrigated agriculture northeast of Lethbridge, Alberta (Figure 2). The region has a semi-arid continental climate due to its location in the rain shadow of the Rocky Mountains (Table I). Extreme temperature variability is common during the winter months due to warm dry Chinook winds that frequently occur in the area. Although most of the precipitation occurs during the summer months, the majority of overland flow occurs in early spring, when the soils are frozen. During the summer months, the majority of precipitation is easily absorbed by the regions Mollisol (Chernozemic) soils.

Watersheds were delineated for three water-quality sampling sites: Szietna, Piyami, and Battersea Drains (Figure 2 and Table II). The outlet for each of these watersheds is located in irrigation return-flow drainages of

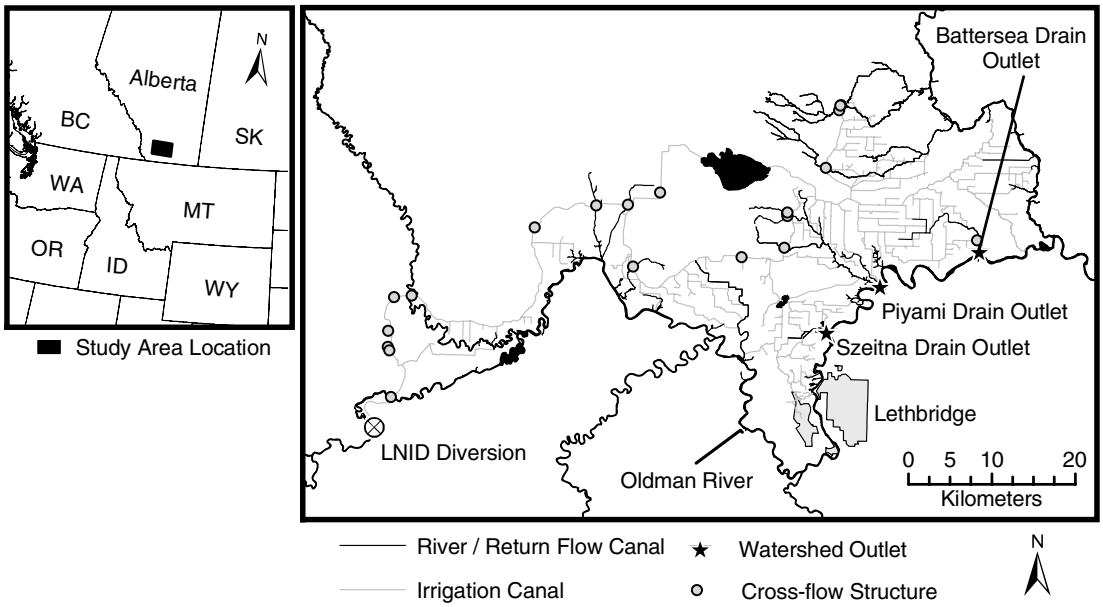

Figure 2. Study area overview

Table I. Climate normals (1971–2000) at Lethbridge, Alberta (station number 3 033 880) (Environment Canada, 2002)

Parameter	Jan	Feb	Mar	Apr	May	Jun	Jul	Aug	Sep	Oct	Nov	Dec
Maximum temperature (°C)	−1·8	1·5	6·0	12·9	18·2	22·3	25·5	25·4	20·1	14·0	4·3	−0·2
Minimum temperature (°C)	−13·8	−10·7	−6·5	−0·9	4·2	8·6	10·5	100·0	5·1	0·0	−7·2	−12
Precipitation (mm)	17·6	11·6	24·0	31·3	53·5	63·0	47·5	45·8	39·6	18·9	16·9	16·7

Table II. Topographic characteristics of the study watersheds

Watershed	Elevation range (m)	Average slope (°)	Maximum slope (°)
Szietna Drain	102	1·0	19·8
Piyami Drain	230	1·1	28·7
Battersea Drain	72	0·7	7·0

the Lethbridge Northern Irrigation District (LNID). Prior to anthropogenic disturbances, the runoff-contributing areas of Szietna, Piyami, and Battersea Drains were approximately 21 km^2, 258 km^2 and 63 km^2 respectively. In contrast to Piyami Drain, which naturally contained an intermittent stream with a drainage density of approximately 0·2 km km^{-2}, the Szietna and Battersea drainages were not free flowing prior to irrigation infrastructure. Containing approximately 680 km of irrigation canals, the LNID has imposed an artificial drainage density of 1·4 km of canal per square kilometre in the study area.

Elevation data were provided by AltaLIS, the agent for Spatial Data Warehouse, which is a not-for-profit organization maintaining and promoting Alberta's digital mapping. These elevation data sets are available in a 100 m regular grid with many additional surface-specific point elevations to define the framework of the terrain, including spot heights and points along ridges, streams, and saddles. The elevation point density for the study area ranges from 103 km^{-2} in the low-relief eastern area to 850 km^{-2} in the more rugged western foothills region (Kienzle, 2004). From this data set, a DEM with a 20 m grid cell size was generated using the TOPOGRID command in ArcInfo™. Details of the DEM generation process are described in Kienzle (2004).

Flow-path modelling pre-assessment

Schneider (2001) stated that it is crucial to identify the properties a DEM must possess before a DEM-based model can be successfully implemented. An initial assessment was carried out to determine (a) which features in the landscape affect overland flow paths, (b) whether a DEM created from the available data set represents the hydrologically significant terrain features, and (c) which new procedures may be required to incorporate additional data to ensure appropriate representation of the hydrologically significant terrain features.

Between the years 1908 and 1998, Lethbridge, Alberta, received an annual average rainfall of 265 mm (Environment Canada, 1998). In June 2002, over 140 mm of rain fell in three consecutive days, effectively saturating the soils in the region. In-field observations of runoff patterns during this time indicated that roads, ditches, culverts, and irrigation canals significantly influenced overland flow pathways. Because these features are frequently misaligned with the naturally occurring topographic aspect, they enforce anthropogenic drainage patterns. The low-relief topography in the study area exacerbates the impact of the anthropogenic runoff rerouting, leading to significant deviations from the drainage patterns that naturally predominated (Figure 3). The spring flood also demonstrated that irrigation canals increase the effective drainage density of nearby streams by capturing runoff. Although natural depressions in most landscapes are relatively uncommon (O'Callaghan and Mark, 1984), potholes in glaciated terrain and depressions caused by the construction of roads are commonplace (Band, 1986; Duke *et al*., 2003). During the spring flood, these depression features accumulated runoff that eventually infiltrated into the soil or evaporated into the atmosphere. At some of these road-induced depression locations, culverts have been installed that facilitate the progression of runoff towards irrigation canals or natural drainage networks. Although the majority of research previously completed on the hydrological effects of roads was not conducted in the northern Great Plains (e.g. Montgomery, 1994; Wemple *et al*., 1996; Jones *et al*., 2000; Dijck, 2000; La Marche and Lettenmaier, 2001; Tague and Band, 2001; Nyssen *et al*., 2002), these observations indicate that the combination of roads, culverts, and irrigation canals may also influence intra-watershed transport, the size and shapes of watersheds, and the stream water quantity, quality, and runoff response in the grasslands region of southern Alberta.

The point-elevation data set, provided by AltaLIS, lacked sample points along roads, ditches, and many irrigation canals. A comparison between field elevation surveys of 52 road cross-sections and the DEM with

Figure 3. Runoff flowing along the topographic slope, from the field towards the road, is deflected 90° by a secondary highway. Most roads in southern Alberta are raised to reduce the potential for snowdrift during winter (Duke *et al*., 2003)

a 20 m grid cell size indicated that the photogrammetrical sampling of elevation points were too coarse to represent the terrain complexity associated with roads and other hydrologically significant features that are sufficiently large to cause surface runoff rerouting. The inadequacy of the point-elevation data set to sample road, ditch, and canal features will, therefore, inevitably lead to incorrect overland flow patterns. In regions with low-relief terrain, such as the grassland in southern Alberta, this would impede the accurate identification of potential pollution sources. It is this incompatibility of scales that poses significant challenges to hydrological simulations, as stated by Moore *et al*. (1991), and Band and Moore (1995).

Based on the assessment of the requirements to model overland flow pathways accurately in the study area, it was determined that (a) irrigation canals must be explicitly enforced in the flow-direction matrix to ensure the simulated flow paths do not inaccurately intersect and cross them, (b) roads and ditches must be enforced into the flow-direction matrix as a function of the cross-sectional profile of the road, (c) split-flow (diversion) patterns resulting from branching irrigation canals must be permitted and incorporated into the watershed delineation procedure, and (d) culverts must be explicitly enforced in the model because their presence facilitates the progression of runoff across roads; the absence of culverts also results in the formation of dead drainages.

Description of RIDEM

A stand-alone computer program was developed that enables the integration of ancillary data including roads, ditches, culverts and canals into the process of flow direction determination. A more realistic overland drainage pattern is produced, enabling the improved delineation of watersheds and potential pollution sources. RIDEM manipulates grid-based overland flow paths using the D8 approach (O'Callaghan and Mark, 1984). RIDEM has two main components: an REA, and a CEA. The REA is described in detail by Duke *et al*. (2003) and is summarized briefly below. The CEA is a new component, which, when combined with the REA, allows the improved representation of overland flow paths within an anthropogenically modified landscape containing roads, ditches, culverts and irrigation canals.

The REA

The REA enables the integration of ancillary data, such as road elevations, ditch depths, and culvert locations, into the process of flow direction determination (Duke *et al*., 2003). The ancillary data are derived

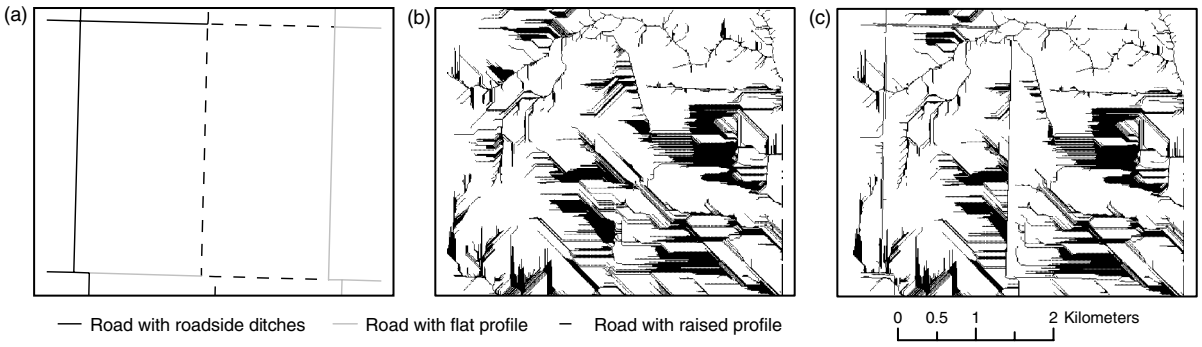

Figure 4. Overland flow-path patterns resulting from the REA (after Duke *et al*. (2003)): (a) a typical road network; (b) D8-derived drainage pattern showing the grid cells with a runoff contributing area greater than 5000 m^2, in black; (c) REA-derived drainage pattern showing the grid cells with a runoff contributing area greater than 5000 m^2, in black

either from existing digital databases or from field surveys. The REA reroutes overland flow paths derived using the D8 algorithm (O'Callaghan and Mark, 1984) according to road cross-sectional attribute and culvert information. The resulting drainage paths are considerably more precise than flow paths derived conventionally. The effect of the REA on overland flow paths is illustrated in Figure 4, where the roads act as barriers to the predominantly west-to-east overland flow patterns derived using the conventional D8 algorithm. The REA also identifies depression areas next to roads that can cause the formation of dead drainages.

The CEA

The CEA component of RIDEM imposes the known flow directions within irrigation distribution systems on a DEM-derived drainage network in D8 format (O'Callaghan and Mark, 1984). The CEA integrates the principles of both cross-flow and split-flow patterns common in irrigation canal networks, which may substantially alter the runoff contributing areas of a watershed.

Enforce stream drainage patterns. In this step of the CEA, the grid cells representing streams are routed off the edge of the grid cell matrix. Processing proceeds from the most downstream grid cells, located on the edge of the grid matrix, to each adjoining grid cell that represents a stream. The output of this process is a flow-direction layer that conforms spatially to the known stream course locations. Utilizing ancillary stream data in this manner has the same effect as the 'stream burning' process (Saunders, 2000), without the disadvantage of introducing routing errors when sinks (DEM depressions) are encountered (Saunders, 2000).

Enforce canal flow directions. Starting with the canal intake grid cell, all cells are routed downstream from lower to higher order canals (from canal main lines to smaller capacity laterals). The algorithm processes canal grid cells in a downstream direction until all canal grid cells for a particular canal segment have been processed and one of the following three conditions is met: the canal ends, but is linked to another canal; the canal ends, but is linked to a stream; the canal ends without a canal or stream linkage. If the canal ends without linking to either a canal or a stream, the grid cell is flagged as a dead-end canal grid cell (depicted as 'A' in Figure 5). How water is routed from dead-end grid cells, without introducing circular drainage patterns, is discussed in the Assign dead-end grid cells a flow direction section. If the canal ends but is linked to a stream, then a flow direction is assigned into the stream (depicted as 'B' in Figure 5). Canal-to-stream linkages enable return flows within an irrigation canal network. If the canal ends but is linked to a canal of equal or lower order, then a flow direction is assigned into the adjacent canal (depicted as 'C' in Figure 5). At this point, a single flow direction is defined for each canal grid cell, referred to as the main flow direction.

In addition to defining the main flow direction for each grid cell representing a canal, alternate flow directions are logged for the grid cells at canal junction locations. Canal junctions are identified by searching

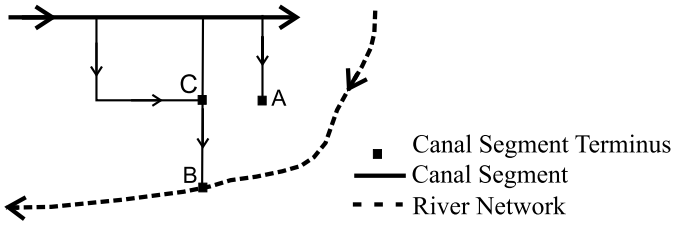

Figure 5. Canal segment links: 'A' signifies a dead-end, 'B' is linked to a stream, and 'C' is linked to another canal

for connecting laterals within a 3 × 3 grid cell window of each canal segment. As each canal junction is identified, alternate flow directions are determined that route flow into the higher order canal segments. A log file is created that contains the locations of the junctions and the alternate flow directions. Both the main and alternate flow directions are used at each canal junction location during the watershed delineation process.

Combine flow direction grids. The enforced stream and canal drainage networks are imposed onto the DEM-derived D8-drainage pattern, creating a single flow-direction matrix. Following the compilation of the three flow-direction matrices, a check is performed to ensure erroneous cross-flow patterns are not produced. Cross-flow patterns result when attempting to enforce flow along linear features that do not include cardinal neighbours in the raster representation (Figure 1). Cross-flow patterns would result in overland flow progressing from the natural landscape across grid cells representing irrigation canal segments. Thus, the cross-flow check ensures irrigation canal segments and the stream networks capture overland flow from adjacent cells.

Assign dead-end grid cells a flow direction. The grid cells representing dead-ends in the canal network are temporarily assigned a flow direction from the DEM-derived D8-flow direction matrix. A check is performed to determine whether the DEM-derived flow direction introduces an endless loop. In grid-based modelling, all grid cells must drain to the edge of the DEM matrix (Jensen and Domingue, 1988). If a loop is identified, then the algorithm steps back along the canal, one grid cell at a time, starting with the terminus grid cell, and locates the first DEM-derived flow direction that does not produce a loop. Once this grid cell has been identified, all flow from the canal segment is rerouted out of the canal through this grid cell. This process can produce flow patterns within a canal segment where water flows in the wrong direction. However, the restriction of a continuous flow-direction matrix in grid-based hydrological modelling necessitates this compromise. A continuous and topologically correct flow-direction matrix is produced with both the stream and canal network enforced.

Create cross-flow patterns. At each canal–stream crossing location, the flow directions are manipulated to create a cross-flow pattern, thereby simulating a siphon, flume, or culvert structure (Figure 1). Cross-flow drainage patterns in grid-based modelling allow the natural progression of runoff in drainage courses while maintaining the enforcement of flow directions within canal segments.

Delineate watershed. The model delineates the upstream contributing area for the grid cell representing the watershed outlet. In contrast to conventional automated watershed algorithms, the CEA takes into account the alternate flow directions at canal junction points that were identified and logged in step two of the CEA. The alternate flow directions are implemented through an iterative delineation process. First, the watershed is derived using conventional methods. Next, the CEA searches for grid cells representing junctions located within a 3 × 3 grid cell window of the watershed boundary. If a canal junction is located next to the watershed boundary, then the alternate flow direction in the log file is assigned at the junction grid cell and the watershed is once again delineated. This process continues until new irrigation canal junction points are not located within

a 3×3 grid cell window of the watershed boundary. The resulting watershed is then representative of the split-flow patterns within the irrigation canal network.

Data collection and processing

Conventional flow-direction routing. Landscape drainage patterns were derived using a conventional grid-based approach. This process involved the so-called 'filling' of local sinks in the DEM, and subsequently deriving the local flow direction for each grid. The D8 flow-direction algorithm was used for this process as implemented in TARDEM, a suite of programs for the analysis of digital elevation data (Tarboton, 1997). TARDEM's implementation of the D8 algorithm is identical to the original D8 algorithm introduced by O'Callaghan and Mark (1984) for grid cells that have at least one neighbouring grid cell with a lower elevation. However, the algorithm uses the approach introduced by Garbrecht and Martz (1997) for cells that lack a downslope neighbour. The implementation of the D8 algorithm in TARDEM is referred to as D8-TOPAZ.

REA. The flow-direction matrix output from the conventional process described above was manipulated by enforcing typical road cross-sectional profiles using the REA model (Duke *et al.*, 2003). Approximately 1032 km of gravel roads and paved secondary highways, comprising 440 segments within a geographical information system vector layer, were classified into one of three categories: flat roads; raised roads; and roads with a ditch. Fifty-two road cross-sections were surveyed with a theodolite to determine the average ditch-to-road and ditch-to-field heights within each road category (as defined in Duke *et al.* (2003)). Because the study area contained different road classes, which have different construction templates (Alberta Transportation and Utilities, 1996), the roads were categorized into four individual classes: secondary highway (raised road); secondary highway (road with ditch); local road (raised road); and local road (road with ditch). The mean ditch-to-field and ditch-to-road heights for each category were then used to manipulate the conventional flow-direction matrix with the REA (Table III). Categorizing the roads into the four classes minimized the variation of ditch-to-road and ditch-to-field heights within each category.

A total of 206 culverts located at road intersections were identified and used as an input variable in the REA model. Drainage culverts installed at road intersections were included to enable the REA model to simulate the hydrological linkages between ditch segments more accurately.

CEA. The flow-direction matrix output from the REA was subsequently manipulated with the CEA to account for the distribution system within the irrigation district. This process consisted of enforcing the

Table III. Summary statistics of surveyed ditch-to-road and ditch-to-field heights; mean values used to manipulate the conventional flow-direction matrix are in bold

		Measured height (m)			
		Secondary highway		Gravel road	
		Ditch to field	Ditch to road	Ditch to field	Ditch to road
Raised roads	Mean	—	—	—	**0·919**[a]
	SD	—	—	—	0·462[a]
	Minimum	—	—	—	0·233[a]
	Maximum	—	—	—	2·050[a]
Roads with ditch	Mean	**0·762**	**1·581**	**0·471**	**1·079**
	SD	0·452	0·249	0·262	0·374
	Minimum	0·080	0·895	0·015	0·340
	Maximum	1·930	2·010	1·006	1·773

[a] 'Ditch to road' refers here to the height of the road relative to the adjacent field.

known flow directions within each canal segment, incorporating cross-flow patterns associated with flume and siphon structures, and incorporating divergent flow patterns at canal junctions. Approximately 682 km of irrigation canals were enforced, along with 16 cross-flow structures.

Model verification. Verifying the drainage patterns and watersheds delineated with RIDEM was precluded by several factors. First, a more accurate data set of elevations or watershed boundaries did not exist. Second, the extent of the study area was relatively large (approximately 1400 km^2), prohibiting direct field verification of watershed boundaries. Third, in-field flow-direction determination in some areas was uncertain because the terrain in the study area was relatively flat. The average slope in the study area was 2·4%.

The REA model was, therefore, validated by verifying the locations where runoff was predicted to flow across roads. Because these locations correspond to topographic depressions where runoff may concentrate, it was hypothesized that these locations should contain a drainage culvert to facilitate the progression of runoff. The predicted culvert locations were considered accurate if any one of the following features was located at each location: a culvert, road-side cattails (*Typha latifolia*), runoff ponding, dead vegetation due to the prolonged spring precipitation event in the spring of 2002, a prominent topographic depression, or an irrigation canal. The model was considered in error when a predicted culvert location was not a depression, but instead a ridge or side slope. The CEA component of the model was assumed to be accurate, because the flow directions for each segment coincided with the known flow directions.

Delineation of dead drainages. Ludwig *et al.* (1995) stated that areas with high infiltration capacities or high surface water storage break the hydrological connection between an area in a watershed and the outlet. In southern Alberta, runoff almost never flows overtop of local roads, even in the most extreme precipitation event. Therefore, the upstream contributing area (or watershed) of each predicted runoff road-crossing location that did not contain a culvert was considered a dead drainage. Because this study was intended to determine areas likely to contribute to surface runoff, and thereby potentially influence water quality, these areas were extracted from each watershed. The remaining watershed represents the gross watershed boundaries, excluding dead drainages caused by the construction of roads. The area that remains in each watershed is, therefore, linked to the watershed outlet by a direct drainage pathway. Dead drainage extraction from gross watershed boundaries has been implemented previously to determine effective watershed boundaries (PFRA, 1983), to estimate erosion patterns (Ludwig *et al.*, 1995), and for the development of the third version of the *Digital atlas of the world water balance* (Asante *et al.*, 1999).

RESULTS

Gross watershed boundaries

The shape and spatial arrangement of the gross watersheds derived using RIDEM differed significantly from those delineated with the D8-TOPAZ algorithm (Figure 6). The greatest similarity between the D8-TOPAZ- and the RIDEM-derived watersheds occurred in the Piyami Drain watershed, yet less than half the grid cells (49·4%) were common to both watersheds (Table IV). The comparisons of watershed areas listed in Table IV were calculated using the percentage agreement statistic (Equation (1)). Because a portion of the canal main line was common to each watershed (Figure 6), the area comparisons between the watersheds delineated with D8-TOPAZ and RIDEM were also made excluding this area (Table V).

$$\mathrm{XPA} = \frac{W_{\mathrm{B}}}{W_{\mathrm{D8}} + W_{\mathrm{RIDEM}} + W_{\mathrm{B}}} \times 100 \tag{1}$$

where XPA (%) is the watershed agreement, W_{B} (km^2, or number of grid cells) is the area delineated by both the D8-TOPAZ and the RIDEM algorithms, W_{D8} (km^2, or number of grid cells) is the area delineated by the

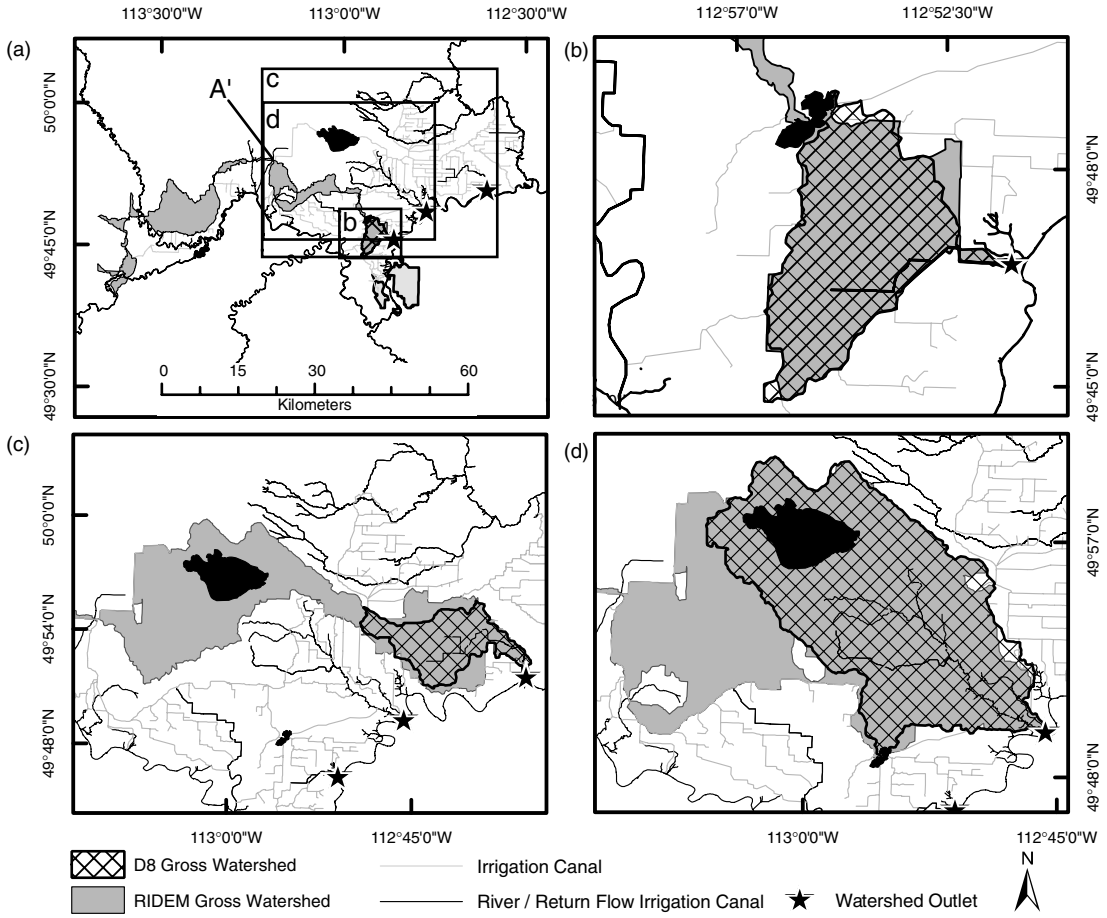

Figure 6. Gross watershed boundaries using the D8 algorithm and RIDEM. (a) Overview map of the Szeitna Drain watershed, showing the area common to all three watersheds along the canal mainline. The common area includes the grey area west of the point labelled A'. (b) Inset of Szeitna Drain. (c) Inset of Battersea Drain. (d) Inset of Piyami Drain

Table IV. Gross watershed area comparisons

Watershed	Watershed area (km^2)		Agreement (%)
	D8-TOPAZ	RIDEM	
Szeitna Drain	21·5	207·0	10·0
Piyami Drain	257·9	504·7	49·4
Battersea Drain	63·0	405·1	15·3

D8-TOPAZ algorithm only, and W_{RIDEM} (km^2, or number of grid cells) is the area delineated by the RIDEM algorithm only.

Dead drainages

RIDEM predicted 647 locations where runoff would theoretically cross a road. Of the 647 predicted culvert locations, 275 (43%) contained a culvert or irrigation canal, 495 (77%) showed direct evidence for model

Table V. Gross watershed area comparisons, excluding the area common to all three watersheds along the irrigation canal mainline

Watershed	Watershed area (km^2)		Agreement (%)
	D8-TOPAZ	RIDEM	
Szeitna Drain	21·5	74·2	27·7
Piyami Drain	257·9	371·9	66·7
Battersea Drain	63·0	272·4	17·9

Table VI. Hydrologically linked watershed areas

Watershed	Watershed area (km^2)		Amount of gross watershed hydrologically linked (%)
	Gross watershed	Hydrologically linked	
Szeitna Drain	207·0	138·1	66·7
Piyami Drain	504·7	322·3	63·9
Battersea Drain	405·1	265·0	65·4

verification (see Model verification section), 70 (11%) locations showed neither evidence to confirm the model nor evidence to suggest model error, and 82 (13%) were considered erroneous. The uncertainty of the 70 locations was due to the presence of extremely flat terrain, making it difficult to judge the appropriateness of the predicted culvert location. Extracting road-induced dead drainages also significantly reduced the watershed area for each water-quality sampling station (Table VI), making the hydrologically linked watersheds convoluted and patchy (Figure 7).

DISCUSSION

The differences between the gross watershed areas derived using the conventional D8-TOPAZ flow direction algorithm and RIDEM indicate that rural infrastructure (including roads, ditches, culverts, irrigation canals, siphons, and flumes) significantly influences the size and shape of watersheds in the study area. In fact, the watershed area discrepancies are much larger than those reported here, because the area comparisons did not include the headwaters of the Oldman River, which is the source of irrigation water in the LNID. For example, the percentage agreement between the D8-TOPAZ and RIDEM watersheds for Piyami Drain, including the headwaters of the Oldman River, was 3·7%.

The gross watershed boundaries delineated with RIDEM were atypical of prairie watersheds unaffected by anthropogenic disturbances. Instead of forming shapes similar to water drops, the watersheds became comprised of fragmented areas linked by the irrigation canal network. In contrast, the watershed boundaries derived with the D8-TOPAZ flow-direction algorithm were much more typical of prairie watersheds before rural infrastructure was built (Figure 6). The watersheds derived with the D8-TOPAZ algorithm are likely to coincide with the watershed boundaries prior to the construction of roads and irrigation canals for two reasons:

1. The DEM was more representative of terrain prior to the construction of roads, ditches, culverts and irrigation canals because the sampling interval of the elevation points used to interpolate the DEM was too coarse to include rural infrastructure. This is also likely the case with most DEMs available through government agencies, which were created to give a general representation of the terrain over a large area.

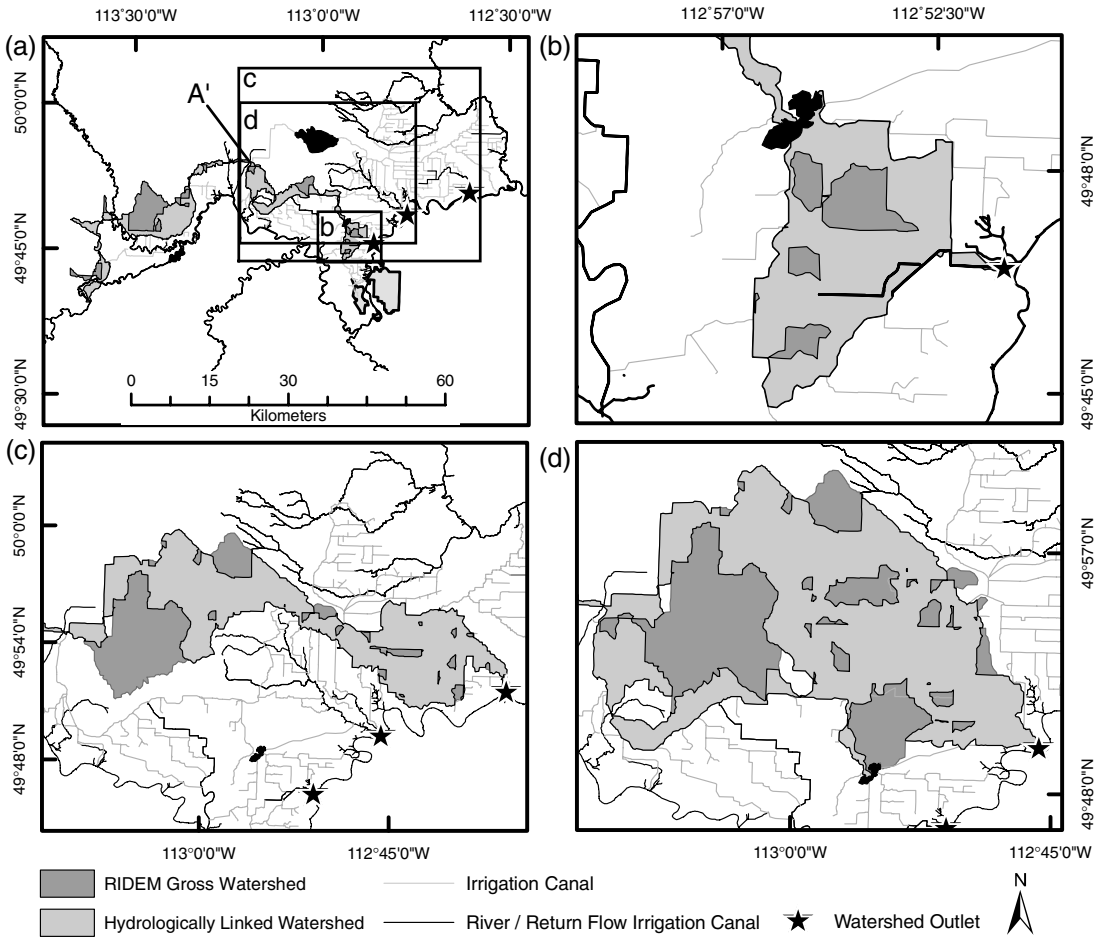

Figure 7. Gross and hydrologically linked watershed boundaries derived using RIDEM. (a) Overview map of the Szeitna Drain watershed, showing the area common to all three watersheds along the canal mainline. The common area includes the grey areas west of the point labelled 'A'. (b) Inset of Szeitna Drain. (c) Inset of Battersea Drain. (d) Inset of Piyami Drain

2. The conventional grid-based flow-direction algorithm D8-TOPAZ was not designed to model the split-flow patterns that occur within the distribution system of the LNID. Therefore, the D8-TOPAZ algorithm is not applicable in irrigated landscapes, but would be representative of flow paths in a natural setting.

Although irrigation canals affected the gross watershed boundaries, roads influenced intra-watershed transport, significantly affecting the portion of the gross watersheds linked to the outlet by a direct drainage pathway (e.g. Figure 4). The consistency between the locations where runoff was predicted to cross a road (647) and observations made in the field verified the accuracy of the drainage modifications made by the REA (77% of predicted road breach locations were accurate). Because a portion of the canal mainline was common to each watershed, and the topography in each watershed is similar, the proportion of each gross watershed linked to the outlet was nearly equal (Table VI). The hydrologically linked watershed maps also indicated that remote areas of the watershed are adequately linked to the watershed outlet, potentially influencing water quality. In contrast, areas directly adjacent to a stream channel may be disconnected from the watershed outlet by the presence of roads that act as barriers to overland flow. As a result, remote areas of the watershed may

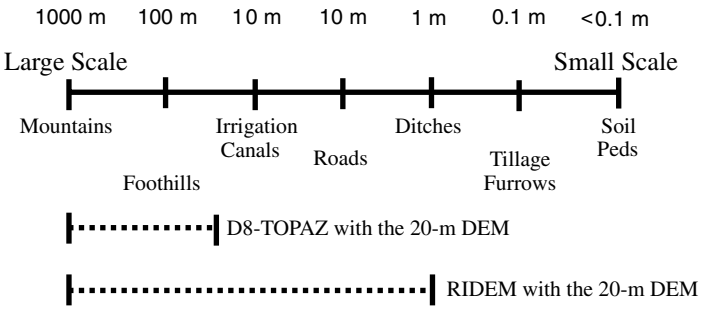

Figure 8. Topographic feature size of hydrologically significant terrain features successfully modelled with the conventional D8 flow-direction algorithm versus RIDEM using the 20 m elevation data set in this study

be significant sources of pollution, equal to or even greater than areas immediately adjacent to stream courses, when rural infrastructure is present.

The sensitivity of the watersheds to rural infrastructure indicated that the scale of the DEM was insufficient to delineate the watersheds accurately using a conventional grid-based flow-direction algorithm. This conclusion supports the previous findings regarding the tendency of grid-based runoff routing models to produce grossly simplified drainage patterns (Moore *et al*., 1991; Band and Moore, 1995; Schneider, 2001). The incorporation of ancillary data reduced the scale of runoff transport pathways modelled below the scale represented by the DEM (Figure 8).

Downscaling overland flow paths with RIDEM would also significantly affect the results of analysing the flow path distance of suspected pollution areas to streams. This type of spatial analysis has been used previously to characterize the vulnerability of surface water to pollution (Endreny and Wood, 1999; Heathewaite *et al*., 2000; Cooke *et al*., 2002; Endreny, 2002; Tian *et al*., 2002).

Band and Moore (1995) described the development of fully distributed parameter hydrological models as little more than 'academic exercises', in part because of difficulties collecting terrain data of sufficient detail to characterize a watershed. The flow-direction matrices derived using RIDEM could be incorporated into existing grid-based models to enhance the scale of runoff transport process. Models such as ANSWERS (Areal Nonpoint Source Watershed Environment Response Simulation; Bouraoui and Dillaha, 2000), TOPLATS (Topographically-based Land–Atmosphere Transfer Scheme; Famiglietti and Wood, 1994), or GRISTORM (Grid-based Variable Source Area Storm Runoff Model; Kim and Steenhuis, 2001) could be used to determine event-based effective watershed areas. Alternatively, simpler models that utilize grid-based flow-direction matrices, such as the Contributing Area–Dispersal Area (CADA) Export Coefficient (EC) model (Endreny, 2002) could be implemented to determine locations where pollutant loads enter local receiving waters. Models that simulate the transport of bacteria, such as presented by Tian *et al*. (2002), could also benefit from the improved surface flow paths provided by RIDEM.

Although it may be argued that the inadequate representation of rural infrastructure within the DEM was due to an insufficient horizontal grid cell size, in actuality it was the sampling interval of the original photogrammetric elevation points that ultimately restricted the landscape features that were expressed in the DEM (Zhang and Montgomery, 1994; Gao, 1998; Gong *et al*., 2000; Huang, 2000; Kienzle, 2004). Therefore, incorporating ancillary data to derive overland flow paths accurately at the desired scale was a necessity. High-resolution DEMs, acquired using technologies such as LIDAR, will likely alleviate the inadequacy of the grid-data structure to represent terrain features as large as irrigation canals, roads, and ditches. Consequently, these high-resolution data sets enable smaller scale analysis using conventional flow-direction algorithms. However, until high-resolution data sets are both practical (from data storage and processing perspectives) and cost effective, ancillary data models such as RIDEM will remain an important tool to overcome the inadequacies of the grid-data structure and conventional flow-direction algorithms.

CONCLUSIONS

The results of this study show that RIDEM can be used to downscale grid-based drainage patterns accurately. Because the model incorporates commonly available ancillary data (viz. roads, ditches, irrigation canals, culverts, siphons, and flumes), the implementation of the model is practical and economical. The potential of RIDEM may, therefore, extend beyond the identification of potential water-pollution source areas. The model may also have the potential to aid in erosion prediction, soil moisture modelling, pest forecasting, crop yield forecasting, and many other applications.

Based on the differences between the gross watersheds derived using the conventional D8-TOPAZ flow-direction algorithm and RIDEM, two major conclusions were derived:

1. When regional scale DEMs do not represent rural infrastructure, overland flow patterns derived with conventional grid-based flow direction algorithms are oversimplified.
2. Conventional flow-direction algorithms, such as D8-TOPAZ, were not designed to predict watershed structure accurately in irrigated landscapes and remain unsuitable in regions with significant irrigation infrastructure.

Field observations showed that several small ditches and return flow channels that were located in the study area were not included in the irrigation district's database. Considering the effects imposed on the landscape drainage patterns by irrigation canals, these features would need to be incorporated into the canal database to maximize the accuracy of the simulated drainage paths. Several workers have argued against discretized flow-direction algorithms, including D8-TOPAZ, claiming that algorithms supporting dispersion are more realistic on hillslopes (Freeman, 1991; Quinn *et al*., 1991; Desmet and Govers, 1996; Tarboton, 1997). We suspect that, at the regional scale, the extent of watersheds in this study area is significantly more sensitive to rural infrastructure than the selection of grid-based flow-direction algorithms. Research is currently under way to test this hypothesis. Errors associated with the prediction of road-crossing culvert locations also suggested that some terrain variation was not represented in the DEM. As a result, an elevation point data set collected at a sampling interval of less than 100 m would enable RIDEM to capture smaller scale landscape transitions.

ACKNOWLEDGEMENTS

This research was funded by the National Sciences Engineering and Research Council of Canada (NSERC) and the Canadian Water Network, whose support is greatly appreciated. Thanks are due to Kevin Haggert and Kevin Morris of the LNID for their valuable knowledge of the study area and provision of canal infrastructure data. We also would like to acknowledge the facilities provided by the University of Lethbridge.

REFERENCES

Alberta Transportation and Utilities. 1996. *Highway geometric design guide*. Government of Alberta, Edmonton, Alberta.

Asante K, Olivera F, Maidment D, Famiglietti J. 1999. *Digital atlas of the world water balance*, version 3·0. Center for Research in Water Resources, The University of Texas at Austin, Austin, TX.

Band LE. 1986. Topographic partition of watersheds with digital elevation models. *Water Resources Research* **22**: 15–24.

Band LE, Moore ID. 1995. Scale landscape attributes and geographical information systems. In *Scale issues in Hydrological Modelling*, Kalma JD, Sivapalan M (eds). Wiley: Toronto, Ontario; 159–179.

Beven K. 1995. Linking parameters across scales: subgrid parameterization and scale dependent hydrological models. *Hydrological Processes* **9**: 507–525.

Bouraoui F, Dillaha TA. 2000. ANSWERS-2000: non-point-source nutrient planning model. *Journal of Environmental Engineering* **126**: 1045–1055.

Cerdan O, Souchere V, Lecomte V, Couturier A, Le Bissonnais Y. 2001. Incorporating soil surface crusting processes in an expert-based runoff model: sealing and transfer by runoff and erosion related to agricultural management. *Catena* **46**: 189–205.

Cooke SE, Mitchell P, Roy L, Gammie L, Olson M, Shepel C, Heitman TL, Hiltz M, Jackson B, Stanley S, Chanasyk D. 2002. *Relationship between beef production and waterborne parasites (* Cryptosporidium *spp. and* Giardia *spp.) in the north Saskatchewan River basin, Alberta, Canada*. Alberta Agriculture, Food and Rural Development, Edmonton, Alberta.

Costa-Cabral MC, Burges SJ. 1994. Digital elevation model networks (DEMON): a model of flow over hillslopes for computation of contributing and dispersal areas. *Water Resources Research* **30**: 1681–1692.

Desmet PJJ, Govers G. 1996. Comparison of routing algorithms for digital elevation models and their implications for predicting ephemeral gullies. *Geographic Information Systems* **10**: 311–331.

Dijck SV. 2000. In *Effects of agricultural land use on surface runoff and erosion in a Mediterranean area*. University of Utrecht, Netherlands.

Duke G, Kienzle SW, Johnson D, Byrne J. 2003. Improving overland flow routing by incorporating ancillary road data into digital elevation models. *Journal of Spatial Hydrology* **3**(2): 27.

Endreny TA. 2002. Forest buffer strips mapping the water quality benefits. *Journal of Forestry* 35–40.

Endreny TA, Wood EF. 1999. Distributed watershed modeling of design storms to identify nonpoint source loading area. *Journal of Environmental Quality* **28**: 388–397.

Environment Canada. 1998. *Canadian daily climate data*, CDCD V1·01. Climate Information Branch, Atmospheric Environmental Service, Ottawa, Ontario.

Environment Canada. 2002. Canadian Climate Normals or Averages 1971–2000. http://www.climate.weatheroffice.ec.gc.ca/climate_normals/index_e.html [February 2004].

Famiglietti JS, Wood EF. 1994. Application of multiscale water and energy balance models on a tallgrass prairie. *Water Resources Research* **30**: 3061–3078.

Freeman TG. 1991. Calculating catchment area with divergent flow based on a regular grid. *Computers & Geosciences* **17**: 413–422.

Gallant JC, Wilson JP. 1996. TAPES-G: a grid-based terrain analysis program for the environmental sciences. *Computers & Geosciences* **22**: 713–722.

Gao J. 1998. Impact of sampling intervals on the reliability of topographic variables mapped from grid DEMs at a micro-scale. *Geographic Information Science* **12**: 875–890.

Garbrecht J, Martz LW. 1997. The assignment of drainage direction over flat surfaces in raster digital elevation models. *Journal of Hydrology* **193**: 204–213.

Gong J, Li Z, Zhu Q, Sui H, Zhou Y. 2000. Effects of various factors on the accuracy of DEMs: an intensive experimental investigation. *Photogrammetric Engineering & Remote Sensing* **66**: 1113–1117.

Heathwaite L, Sharpley A, Gburek W. 2000. A conceptual approach for integrating phosphorus and nitrogen management at watershed scales. *Journal of Environmental Quality* **29**: 158–166.

Huang YD. 2000. Evaluation of information loss in digital elevation models with digital photogrammetric systems. *Photogrammetric Record* **16**: 781–791.

Hutchinson MF. 1989. A new procedure for gridding elevation and stream line data with automatic removal of spurious pits. *Journal of Hydrology* **106**: 211–232.

Hutchinson MF, Dowling TI. 1991. A continental hydrological assessment of a new grid based digital elevation model of Australia. *Hydrological Processes* **5**: 45–58.

Hyland R, Byrne J, Selinger B, Graham T, Thomas J, Townsend I, Gannon V. 2003. Spatial and temporal distribution of fecal indicator bacteria within the Oldman River basin of southern Alberta, Canada. *Water Quality Resources Journal of Canada* **38**: 15–32.

Jensen SK, Domingue JO. 1988. Extracting topographic structure from digital elevation data for geographic information system analysis. *Photogrammetric Engineering and Remote Sensing* **54**: 1593–1600.

Johnson JYM, Thomas JE, Graham TA, Townshend I, Byrne J, Selinger BL, Gannon VPJ. 2003. Prevalence of *Escherichia coli* o157:H7 and *Salmonella* spp. in surface waters of southern Alberta and its relation to manure sources. *Canadian Journal of Microbiology* **49**: 326–335.

Jones JA, Swanson FJ, Wemple BC, Snyder KU. 2000. Effects of roads on hydrology, geomorphology, and disturbance patches in stream networks. *Conservation Biology* **14**: 76–85.

Kienzle SW. 2004. The effect of DEM raster resolution on first order, second order and compound terrain derivatives. *Transactions in GIS* **8**: 83–111.

Kim SJ, Steenhuis TS. 2001. GRISTORM: grid-based variable source area storm runoff model. *Transactions American Society of Agricultural Engineering* **44**: 863–875.

La Marche JL, Lettenmaier DP. 2001. The effects of forest roads on flood flows in the Deschutes River, Washington. *Earth Surface Process and Landforms* **26**: 115–134.

Lea NL. 1992. An aspect driven kinematic routing algorithm. In *Overland Flow: Hydraulics and Erosion Mechanics*, Parsons AJ, Abrahams AD (eds). Chapman & Hall: New York, NY; 393–407.

Little JL, Saffran KA, Fent L. 2003. Land use and water quality relationships in the lower Little Bow River watershed, Alberta, Canada. *Water Quality Resources Journal of Canada* **38**: 563–584.

Ludwig B, Boiffin J, Chadoeuf J, Auzet A. 1995. Hydrological structure and erosion damage caused by concentrated flow in cultivated catchments. *Catena* **25**: 227–252.

Montgomery DR. 1994. Road surface drainage, channel initiation, and slope instability. *Water Resources Research* **30**: 1925–1932.

Moore ID, Grayson RB, Ladson AR. 1991. Digital terrain modelling: a review of hydrological geomorphological, and biological applications. *Hydrological Processes* **5**: 3–30.

Nyssen J, Poesen J, Moeyersons J, Luyten E, Veyret-Picot M, Deckers J, Haile M, Govers G. 2002. Impact of road building on gully erosion risk: a case study from the northern Ethiopian highlands. *Earth Surface Processes and Landforms* **27**: 1267–1283.

O'Callaghan JF, Mark DM. 1984. The extraction of drainage networks from digital elevation data. *Computer Vision, Graphics, and Image Processing* **28**: 323–344.

Orlandini S, Moretti G, Franchini M, Aldighieri B, Testa EB. 2003. Path-based methods for the determination of nondispersive drainage directions in grid-based digital elevation models. *Water Resources Research* **39**: 1144.
Prairie Farm Rehabilitation Administration. 1983. *The determination of gross and effective drainage areas in the prairie provinces*. Hydrology Report #104. Prairie Farm Rehabilitation Administration: Regina, Saskatchewan.
Quinn P, Beven K, Chevallier P, Planchon O. 1991. The prediction of hillslope flow paths for distributed hydrological modelling using digital terrain models. *Hydrological Processes* **5**: 59–79.
Rieger W. 1998. A phenomenon-based approach to upslope contributing area and depressions in DEMs. *Hydrological Processes* **12**: 857–872.
Saunders W. 2000. Preparation of DEMs for use in environmental modeling analysis. In *Hydrologic and Hydraulic Modeling Support with Geographic Information Systems*, Maidment D, Djokic D (eds). Environmental Systems Research Institute Inc.: Redlands, CA; 29–51.
Schneider B. 2001. Phenomenon-based specification of the digital representation of terrain surfaces. *Transactions in GIS* **5**: 39–52.
Souchere V, King D, Daroussin J, Papy F, Capillon A. 1998. Effects of tillage on runoff directions: consequences on runoff contributing area within agricultural catchments. *Journal of Hydrology* **206**: 256–267.
Souchere V, Cerdan O, Ludwig B, Le Bissonnais Y, Couturier A, Papy F. 2003. Modelling ephemeral gully erosion in small cultivated catchments. *Catena* **50**: 489–505.
Tague C, Band L. 2001. Simulating the impact of road construction and forest harvesting on hydrological response. *Earth Surface Processes and Landforms* **26**: 135–151.
Takken I, Govers G, Steegen A, Nachtergaele J, Guerif J. 2001a. The prediction of runoff flow directions of tilled fields. *Journal of Hydrology* **248**: 1–13.
Takken I, Jetten V, Govers G, Nachtergaele J, Steegen A. 2001b. The effect of tillage-induced roughness on runoff and erosion patterns. *Geomorphology* **37**: 1–14.
Takken I, Govers G, Jetten V, Nachtergaele J, Steegen A, Poesen J. 2001c. Effects of tillage on runoff erosion patterns. *Soil & Tillage Research* **61**: 55–60.
Tarboton DG. 1997. A new method for the determination of flow directions and upslope areas in grid digital elevation models. *Water Resources Research* **32**: 309–319.
Tian YQ, Gong P, Radke JD, Scarborough J. 2002. Spatial and temporal modeling of microbial contaminants on grazing farmlands. *Journal of Environmental Quality* **31**: 860–869.
Wemple BC, Jones JA, Grant GE. 1996. Channel network extension by logging roads in two basins, Western Cascades, Oregon. *Water Resources Research* **32**: 1195–1207.
Zhang W, Montgomery DR. 1994. Digital elevation model grid size, landscape representation, and hydrologic simulations. *Water Resources Research* **30**: 1019–1028.

